

# Effect of Slip Length on Entropy Generation of Fully Developed Forced Convection in a Micro-Channel for a Power Law Fluid

Vishal Anand and Harikrishnan Lakshmanan

Cyient Limited Hyderabad, Andhra Pradesh

India -500032

vish.anand.iit@gmail.com, harikrishnan.iitm@gmail.com

## ABSTRACT

In this paper, the effect of slip length on entropy generation of fluid flow in a microchannel is analyzed. The flow between the parallel plates is considered fully developed both hydrodynamically and thermally. Uniform heat flux boundary condition is assumed. The fluid is supposed to be non Newtonian, following a power law model. To model the slip, Navier's linear slip law has been used. The spatial distribution of fluid velocity, non dimensional temperature, non dimensional entropy generation and Bejan number has been investigated for different slip length ratios. For dilatants fluids, it is found that that the effect of slip length is significant and cannot be neglected.

## NOMENCLATURE

$A$	Dimensionless Parameter (defined in Eq. 22)
$Br$	Brinkman number
$Be$	Bejan number
$c_p$	Specific heat ( $\text{Jkg}^{-1}\text{K}^{-1}$ )
$k$	Thermal Conductivity ( $\text{Wm}^{-1}\text{K}^{-1}$ )
$l$	Slip Length (nm)
$2L$	Channel Width ( $\mu\text{m}$ )
$n$	Power Law Index
$N$	Non-dimensional Entropy Generation
$p$	Fluid Pressure ( $\text{Nm}^{-2}$ )
$Pe$	Peclet number
$q$	Heat Flux ( $\text{Wm}^{-2}$ )
$\dot{S}$	Entropy Generation Rate ( $\text{WK}^{-1}$ )
$T$	Temperature (K)
$u$	Velocity in x-direction ( $\text{ms}^{-1}$ )
$\bar{u}$	Average Velocity When No-slip at the Wall ( $\text{ms}^{-1}$ )
$x$	Fluid Flow Direction (m)
$y$	Normal to Fluid Flow Direction (m)

## Subscripts

$m$	Mean
$w$	Wall
$RC$	Radial Conduction

<i>AC</i>	Axial Conduction
<i>FF</i>	Fluid Friction
<i>gen</i>	Generation
<i>avg</i>	Average
<i>s</i>	Entropy Generation (WK <sup>-1</sup> )

### Greek Symbols

$\mu$	Consistency Factor (Pa.s <sup>n</sup> )
$\tau$	Shear Stress (Nm <sup>-2</sup> )
$\rho$	Density (kgm <sup>-3</sup> )
$\theta$	Non-dimensional Temperature
$u$	Non-dimensional Velocity in x-direction
$y$	Non-dimensional Channel Width
$\psi$	Dimensionless Heat Flux

## 1. INTRODUCTION

In recent years microfluidics has evolved into an exciting field of study with varied applications in engineering, physics and microbiology. The key application areas of microfluidics include, but are not limited to capillary electrophoresis, enzymatic analysis, DNA analyses, electro-osmotic pumps, inkjet printing and others. In nature and in technology, non Newtonian fluid behavior is so widespread that Newtonian fluid behavior can be regarded as an exception, rather than a rule. The behavior of non Newtonian fluids may be approximated by the power law model. According to this, the fluids with power law index less than 1 are shear thinning (pseudo-plastic) fluids, where the apparent viscosity decreases with strain rate. On the other hand, for shear thickening (dilatant) fluids, the power law index is greater than 1. Here the apparent viscosity increases with increase in strain rate.

The no slip boundary condition, which is almost ubiquitously applied in fluid mechanics is an assumption and cannot be derived from first principles. In fact, for non Newtonian fluids, especially in micro channels, the phenomenon of slip is very significant and has tremendous practical applications.

To model the slip between a surface and fluid, the following equation was first introduced by Navier [1] and later by Maxwell [2]:

$$u_s = l \left. \frac{\partial u}{\partial y} \right|_{wall}$$

Here  $u_s$  is the slip velocity at the surface,  $\frac{\partial u}{\partial y}$  is the derivative of the velocity and  $l$  is the slip length, which is defined as the distance from the surface to the imaginary plane inside the wall, where the extrapolated tangential velocity vanishes. The slip length quantifies the amount of slip and depends on many factors like, wetting properties of the liquid, nature of dissolved gases in the liquid, electrical properties of the liquid, roughness of the surface among others. Application of various slip law models to generalized non Newtonian fluids has been studied in detail by Ferras et al. [3].

The entropy generated in a process or a cycle is related to the lost work by Guoy Studola theorem [4] and hence is an important factor which influences the design of a system for improved efficiency. Mahmud and Fraser [5-6] studied the entropy generated in a pipe as well as in a channel between flat plates for a pressure driven flow of a power law fluid. In their analysis, they neglected viscous dissipation. The effect of viscous dissipation on entropy generation in a flow of a non Newtonian fluid in a circular tube was analyzed by Hung [7].

The slip length affects the velocity distribution in a channel, which in turn affects the temperature distribution and entropy generation in a flow in a channel. Thus it seems appropriate to include the effect of slip length on entropy generation. This paper analyses the effect of slip length on the velocity

distribution, non-dimensional temperature distribution, non-dimensional entropy generation distribution, Bejan number distribution and average entropy generated for a thermally developed flow with viscous dissipation of a power-law fluid in a micro channel. To the best knowledge of the authors, this problem has not been attempted in available literature.

## 2. MATHEMETICAL FORMULATION

Figure 1 shows the schematic representation of flow inside the channel width of  $2L$  with uniform heat flux. The co-ordinate  $x$  represents the flow direction and  $y$  is the normal to the flow direction. The constant heat flux,  $q_w$  is applied on the entire wall. The mathematical formulation is obtained by considering slip on the wall surface.

### 2.1. Velocity distribution

Consider a pressure driven flow of a power law fluid in a 2-Dimensional micro-channel with width  $2L$ , under uniform heat flux boundary conditions. The shear stress relationship for the power-law fluid is as follows;

$$\tau = \mu \left| \frac{du}{dy} \right|^{n-1} \frac{du}{dy} \quad (1)$$

where  $n$  is the power law index. The governing equation for velocity is given

$$\frac{\partial}{\partial y} \left( \mu \left| \frac{du}{dy} \right|^{n-1} \frac{du}{dy} \right) = \frac{dp}{dx} \quad (2)$$

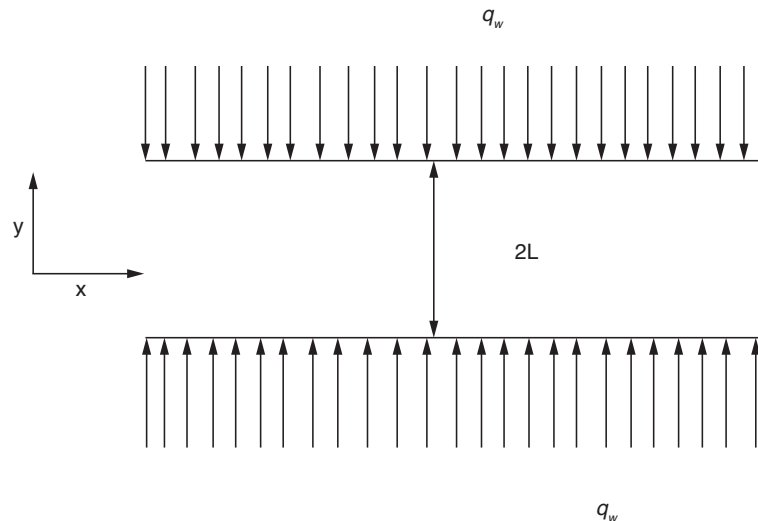


Figure 1. Schematic diagram of the model

The boundary conditions for the Eqn. (2) are as follows;

$$\text{At } y = 0 ; \frac{du}{dy} = 0 \quad (3)$$

$$\text{At } y = \pm L \text{ \& } y = L; u = l \left| \frac{du}{dy} \right| \quad (4)$$

where,

$$\left| \frac{du}{dy} \right| = \frac{du}{dy} \text{ for } -L \leq y \leq 0 \quad (5)$$

$$\left| \frac{du}{dy} \right| = -\frac{du}{dy} \text{ for } 0 \leq y \leq L \quad (6)$$

By solving Eqn. (2) subject to conditions in Eqns. (3-6), the expressions for velocity profile are obtained as:

For  $-L \leq y \leq 0$ ;

$$u = \bar{u} \left( \frac{1}{n} + 2 \right) \left[ \frac{l}{L} + \frac{1}{\frac{1}{n} + 1} - \frac{\left( -\frac{y}{L} \right)^{\frac{1}{n} + 1}}{\frac{1}{n} + 1} \right] \quad (7)$$

For  $0 \leq y \leq L$ ;

$$u = \bar{u} \left( \frac{1}{n} + 2 \right) \left[ \frac{l}{L} + \frac{1}{\frac{1}{n} + 1} - \frac{\left( \frac{y}{L} \right)^{\frac{1}{n} + 1}}{\frac{1}{n} + 1} \right] \quad (8)$$

where  $\bar{u}$  is the average velocity of flow when slip is not considered and is expressed as:

$$\bar{u} = \left( -\frac{1}{\mu} \frac{dp}{dx} \right)^{\frac{1}{n}} \frac{L^{\frac{1}{n} + 1}}{\frac{1}{n} + 2} \quad (9)$$

## 2.2. Temperature distribution

The 2-D energy equation considering viscous dissipation effect (and neglecting axial conduction) of a power law fluid is expressed as:

$$\rho c_p u \frac{\partial T}{\partial x} = k \frac{\partial^2 T}{\partial y^2} + \mu \left| \frac{\partial u}{\partial y} \right|^{n-1} \left( \frac{\partial u}{\partial y} \right)^2 \quad (10)$$

For the uniform heat flux boundary condition, the temperature gradient along the x-direction is written as:

$$\frac{\partial T}{\partial x} = \frac{dT_m}{dx} \quad (11)$$

By substituting Eqn. (11) in Eqn. (10) and for the channel width,  $-L \leq y \leq 0$  (where,  $\left| \frac{\partial u}{\partial y} \right| = \frac{\partial u}{\partial y}$ ) the equation is modified as

$$\rho c_p u \frac{dT_m}{dx} = k \frac{\partial^2 T}{\partial y^2} + \mu \left( \frac{\partial u}{\partial y} \right)^{n+1} \quad (12)$$

There are two independent variables,  $T_m$  and  $T$  in the above equation. So first, an attempt is made to find a value of  $\frac{dT_m}{dx}$  by integrating the Eq. (12).

$$\int_{-L}^0 \rho c_p u \frac{dT_m}{dx} dy = \int_{-L}^0 k \frac{\partial^2 T}{\partial y^2} dy + \int_{-L}^0 \mu \left( \frac{\partial u}{\partial y} \right)^{n+1} dy \quad (13)$$

The first term on RHS of Eqn. (13) is written as

$$\int_{-L}^0 k \frac{\partial^2 T}{\partial y^2} dy = k \frac{dT}{dy} \Big|_{-L}^0 = 0 - (-q_w) = q_w \quad (14)$$

The second term on RHS of Eqn. (13) is simplified as

$$\int_{-L}^0 \mu \left( \frac{\partial u}{\partial y} \right)^{n+1} dy = \mu \left[ \bar{u}^{n+1} \left( \frac{1+2n}{nL} \right)^n \right] \quad (15)$$

Similarly, the LHS of Eq. (13) is written as:

$$\int_{-L}^0 \rho c_p u \frac{dT_m}{dx} = \rho c_p \frac{dT_m}{dx} \bar{u} \left( \frac{1}{n} + 2 \right) \left[ \frac{L}{(1/n+2)} + l \right] \quad (16)$$

Substituting Eqns. (14)-(16) in Eq. 13, the following is obtained:

$$\rho c_p \frac{dT_m}{dx} = \frac{q_w + \mu \left[ \bar{u}^{n+1} \left( \frac{(1+2n)^n}{nL} \right) \right]}{\bar{u} \left( \frac{1}{n} + 2 \right) \left[ \frac{L}{\frac{1}{n} + 2} + l \right]} \quad (17)$$

Substitute Eqn. (17) into Eqn. (12) and the following equation is obtained:

$$\left( \frac{q_w + \mu \left[ \bar{u}^{n+1} \left( \frac{(1+2n)^n}{nL} \right) \right]}{\bar{u} \left( \frac{1}{n} + 2 \right) \left[ \frac{L}{\frac{1}{n} + 2} + l \right]} \right) u = k \frac{\partial^2 T}{\partial y^2} + \mu \left( \frac{\partial u}{\partial y} \right)^{n+1} \quad (18)$$

Thus we see that  $\frac{dT_m}{dx}$  has been eliminated from the energy equation. To solve Eqn. 18, the non-dimensional variables for  $u$ ,  $y$  and  $T$  are introduced. These are represented as:

$$\hat{u} = \frac{u}{\bar{u}}, \hat{y} = \frac{y}{L}, \theta = \frac{k(T - T_w)}{q_w L} \quad (19)$$

After incorporating all the above non-dimensional variables in the Eqn. (18), it is reduced to the following:

$$A \hat{u} = \frac{\partial^2 \theta}{\partial \hat{y}^2} + 2^n Br \left( \frac{\partial \hat{u}}{\partial \hat{y}} \right)^{n+1} \quad (20)$$

where,

$Br$  is the modified Brinkman number for non Newtonian fluids [8] and is given by:

$$Br = \frac{\mu \bar{u}^{n+1}}{q_w (2L)^n} \quad (21)$$

$A$  is given by:

$$A = \frac{n^n + Br 2^n (1+2n)^n}{n^n \left( \frac{1}{\frac{1}{n} + 2} + \frac{l}{L} \right) \left( \frac{1}{n} + 2 \right)} \quad (22)$$

The pertinent boundary conditions are;

$$\hat{y} = 0; \frac{\partial \theta}{\partial \hat{y}} = 0 \tag{23}$$

$$\hat{y} = -1; \theta = 0 \tag{24}$$

Using the above boundary conditions, the Eqn. (20) is solved for  $\theta$  and the final expression for  $\theta$  for the region,  $0 \leq y \leq 0$  is obtained as:

$$\begin{aligned} \theta = \frac{n}{3n+1} & \left[ 2^n Br \left( \frac{2n+1}{n} \right)^n + \frac{A}{\frac{1}{n}+1} \right] \left[ 1 - (-\hat{y})^{\frac{3n+1}{n}} \right] \\ & - \frac{A \left( \frac{1}{n} + 2 \right)}{2} \left[ \frac{l}{L} + \frac{1}{\frac{1}{n}+1} \right] \left[ 1 - (\hat{y})^2 \right] \end{aligned} \tag{25}$$

Similarly, for  $0 \leq y \leq L$ , the procedure from Eqn. (11) to Eqn. (24) can be repeated to yield,

$$\begin{aligned} \theta = \frac{n}{3n+1} & \left[ 2^n Br \left( \frac{2n+1}{n} \right)^n + \frac{A}{\frac{1}{n}+1} \right] \left[ 1 - (-\hat{y})^{\frac{3n+1}{n}} \right] \\ & - \frac{A \left( \frac{1}{n} + 2 \right)}{2} \left[ \frac{l}{L} + \frac{1}{\frac{1}{n}+1} \right] \left[ 1 - (\hat{y})^2 \right] \end{aligned} \tag{26}$$

### 2.3. Entropy generation

The rate of volumetric entropy generation in convection of non-Newtonian fluid is given by [9]:

$$\dot{S}_{gen} = \frac{k}{T^2} \left[ \left( \frac{\partial T}{\partial x} \right)^2 + \left( \frac{\partial T}{\partial y} \right)^2 \right] + \frac{\mu}{T} \left| \frac{\partial u}{\partial y} \right|^{n+1} \tag{27}$$

The non-dimensional entropy generation,  $N_s$  is given by:

$$\begin{aligned} N_s = \frac{\dot{S}_{gen} L^2}{k} & \\ = \frac{\psi^2}{4(1+\psi\theta)^2} & \left[ \left( \frac{\partial \theta}{\partial \hat{y}} \right)^2 + \left( \frac{2}{Pe \times n^n} \right)^2 \left( \frac{n^n + 2^n (2n+1)^n Br}{\left( \frac{1}{n} + 2 \right) \left( \frac{1}{n} + 2 + \frac{l}{L} \right)} \right)^2 \right] \\ & + \frac{Br 2^n \psi}{(1+\psi\theta)} \left| \frac{d\hat{u}}{d\hat{y}} \right|^{n+1} \end{aligned} \tag{28}$$

where,

$$\psi = \frac{q_w L}{k T_w} \quad (29)$$

Dimensionless heat flux,

$$Pe = \frac{\rho c_p \bar{u} L}{k} \quad (30)$$

Peclet number,

Please note that, even though the axial conduction has been neglected in the energy equation, it has *not* been neglected in the entropy generation equation.

In convection, total entropy generation has two components: entropy generation due to heat transfer and that due to fluid friction ( $N_{FF}$ ). Entropy generation due to heat transfer in itself can be divided into entropy generation due to radial conduction ( $N_{RC}$ ) and that due to axial conduction ( $N_{AC}$ ).  $N_{RC}$  depends on the radial gradient of temperature and on the temperature distribution itself.  $N_{AC}$  depends on the axial gradient of the temperature (which is constant for fully developed forced convection) and also on the temperature distribution itself.  $N_{FF}$  depends on the velocity gradient.

In the current study:

$$N_{RC} = \frac{\psi^2}{4(1+\psi\theta)^2} \times \left( \frac{\partial\theta}{\partial\bar{y}} \right)^2 \quad (31)$$

$$N_{AC} = \frac{\psi^2}{4(1+\psi\theta)^2} \times \left( \frac{2}{Pe \times n^n} \right)^2 \left[ \frac{n^n + 2^n (2n+1)^n Br}{\left( \frac{1}{n} + 2 \right) \left( \frac{1}{\frac{1}{n} + 2} + \frac{l}{L} \right)} \right]^2 \quad (32)$$

$$N_{FF} = \frac{Br 2^n \psi}{(1+\psi\theta)} \left| \frac{d\bar{u}}{d\bar{y}} \right|^{n+1} \quad (33)$$

where  $N_{RC}$  accounts for dimensionless entropy generation due to radial conduction;  $N_{AC}$  accounts for dimensionless entropy generation due to axial conduction; and  $N_{FF}$  accounts for dimensionless entropy generation due to fluid friction.

#### 2.4. Bejan number

The dimensionless entropy generation number gives the total entropy generated. But it does not convey which out of two entropy generation mechanisms, namely heat transfer and fluid friction, dominates. To resolve this, Paoletti [10] defined a new number called Bejan number. The Bejan number is the ratio between entropy generated due to heat transfer and total entropy generated. In the current study, it is expressed as :

$$Be = \frac{\frac{\psi^2}{4(1+\psi\theta)^2} \left[ \left( \frac{\partial\theta}{\partial\bar{y}} \right)^2 + \left( \frac{2}{Pe \times n^n} \right)^2 \left[ \frac{n^n + 2^n (2n+1)^n Br}{\left( \frac{1}{n} + 2 \right) \left( \frac{1}{\frac{1}{n} + 2} + \frac{l}{L} \right)} \right]^2 \right]}{N_s} \quad (34)$$

It conveys that when *Be* equals 1, the total entropy generation is due to heat transfer and when *Be* equals 0, the total entropy generation is due to fluid friction.

**2.5. Average dimensionless entropy generation**

The average entropy generation is calculated by integrating the local entropy generation over the width 2L. It is expressed as follows;

$$N_{s,avg} = \frac{1}{2L} \int_{-L}^L N_s dy = \frac{1}{2} \int_{-1}^1 N_s d\hat{y} \tag{35}$$

**3. RESULTS AND DISCUSSION**

The velocity distribution along the channel width is obtained from the Eqns. (7) and (8). The non-dimensional temperature distribution along the channel width is obtained from the Eqns. (25) and (26). The non-dimensional entropy generation along the channel width is obtained from the Eqn. (28). Finally, Bejan number and average dimensionless entropy generation is obtained from the Eqn. (34) and Eqn. (35), respectively. These equations are solved in MATLAB to get the respective distribution of data. Table 1 represents the parameters and their values used in this study.

Brinkman number is the non dimensional representation of the effect of viscous dissipation in the flow. The chosen value of 0.7 conveys that the viscous dissipation has not been neglected in this study. Moreover, this value is consistent with the value used elsewhere in the literature [7].

Figure 2(a) and (b) represent the non-dimensional velocity distribution along the channel width at the different *l/L* (slip length to half channel width) ratio for pseudo plastic (*n* = 0.5) and dilatant fluid (*n* = 2), respectively. For both the cases, the maximum velocity is reached at the centerline, because of symmetric boundary conditions at the walls. The velocity  $\bar{U}$  represents the average velocity of flow when slip is not considered. The non-dimensional velocity is observed to be higher for the higher values of *l/L* ratio.

This is expected because higher slip length means that the slip velocity at the wall is higher which results in higher velocity distribution in the flow. Another way to look at this is that higher slip length means the friction encountered by the flow decreases, so for the same pressure gradient, a higher mass flow rate can be pumped, leading to higher velocity. For *n* = 2, the non-dimensional velocity at the wall are observed to be comparatively higher than for the lower value of power-law index (*n* = 0.5). Moreover, for *n* = 0.5, the non-dimensional velocity variation is observed to be flatter than for *n* = 2. This is because the shear stress at the walls (for the same consistency factor) is higher for a dilatant fluid than for a pseudo plastic fluid. This also explains the fact that the maximum value of non-dimensional velocity is higher for *n* = 2.

Figure 3(a) and 3(b) show the non dimensional temperature distribution along the channel width at different values of *l/L* ratio for pseudo plastic (*n* = 0.5) and dilatant fluid (*n* = 2) respectively. Since the

Table 1. Parameters and their values.

S. No.	Parameter Name	Symbol (Unit)	Value
1	Power-law index	<i>n</i>	0.5 - Pseudo plastic 2 - Dilatant fluid
2	Dimensionless Heat flux	$\psi$	0.1
3	Peclet number	<i>Pe</i>	1
4	Brinkman number	<i>Br</i>	0.7
5	Slip length	<i>l</i> (nm)	10, 500 and 1000
6	Channel Width	2L( $\mu$ m)	100

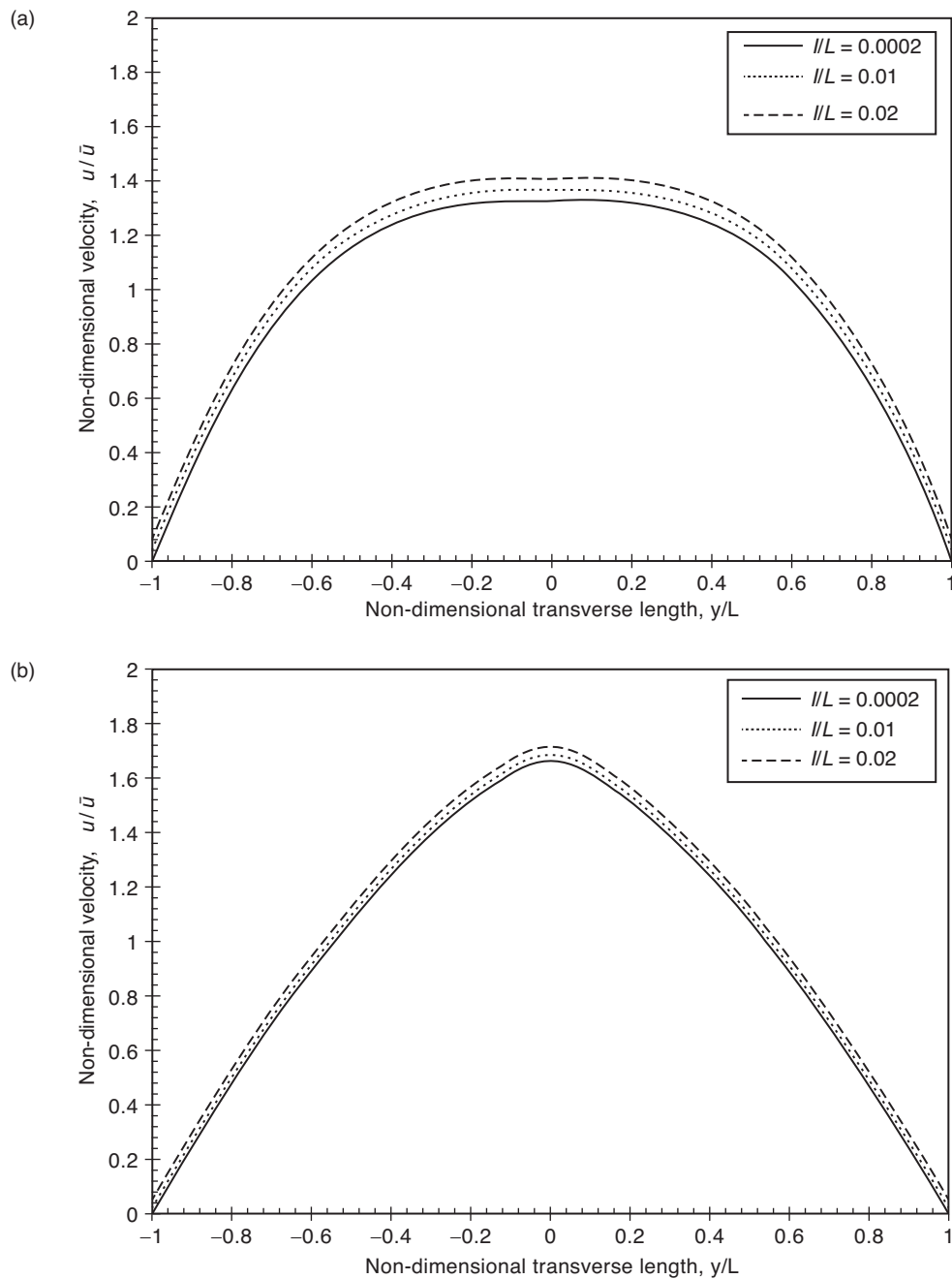


Figure 2. Variation of non-dimensional velocity along the channel width at different  $//L$  ratio for (a)  $n = 0.5$  (b)  $n = 2$

effect of viscous dissipation or  $Br$  has already been studied in literature [7], the  $Br$  has been taken as constant ( $= 0.7$ ) in our analysis. As shown, the slope for the curve is steeper for  $n = 2$  than for  $n = 0.5$ . This is corroborated by Hung [7] for no slip boundary condition. Moreover, as the non dimensional slip length increases, the dimensionless temperature increases. This is because an increase in  $//L$  causes the

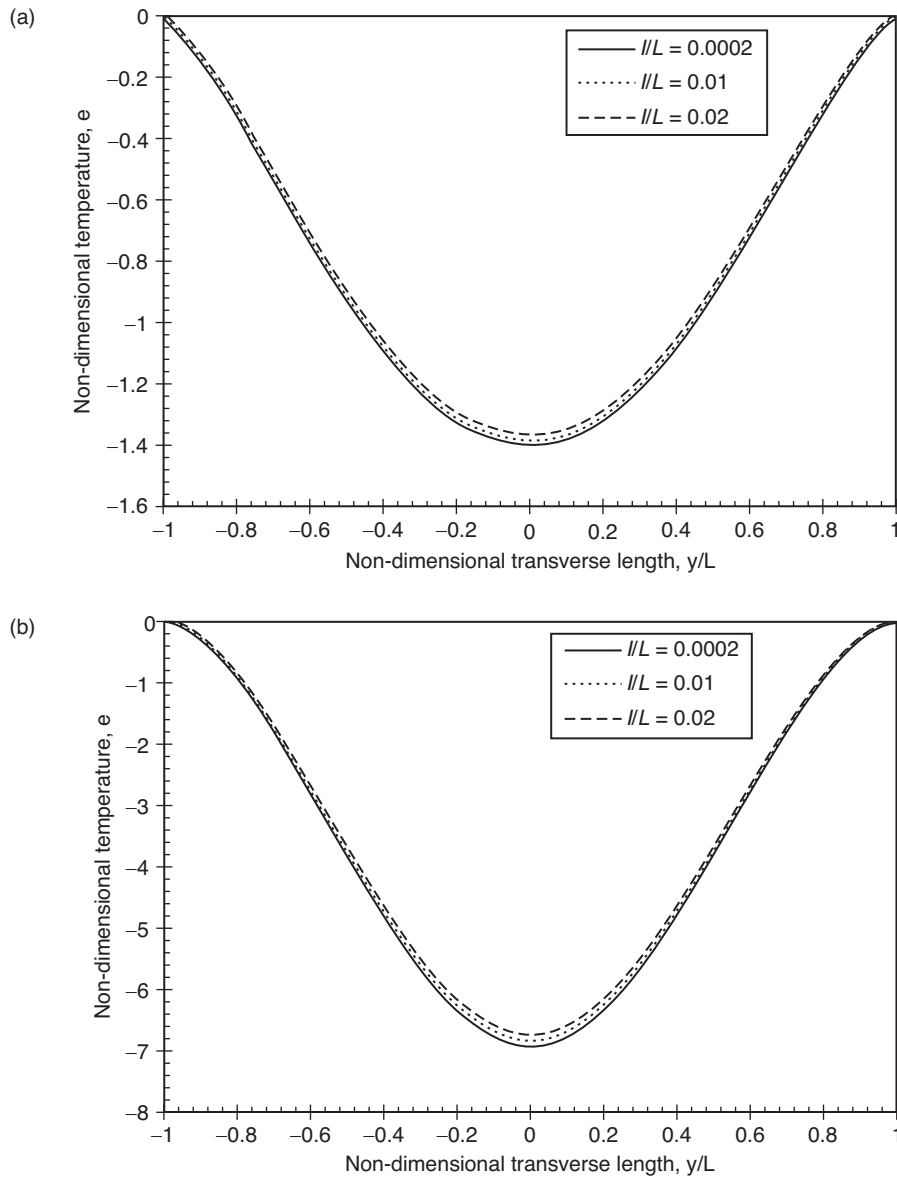


Figure 3. Variation of non-dimensional temperature along the channel width at different  $//L$  ratio for (a)  $n = 0.5$  (b)  $n = 2$

$du/dy$  to increase (see Figure 2), which leads to an increase in heat generation due to viscous dissipation and hence the temperature of the fluid increases.

Figure 4(a) and 4(b) show the non dimensional entropy generation along the channel width at different values of  $//L$  ratio for pseudo plastic ( $n = 0.5$ ) and dilatant fluid ( $n = 2$ ), respectively. The Fig. 4(a) shows for pseudo plastic fluids ( $n = 0.5$ ),  $N_s$  is minimum at the centre, while it is highest at the walls. This is because the radial temperature gradient (and hence  $N_{RC}$ ) and the velocity gradient (and hence  $N_{FF}$ ) are lowest ( $= 0$ ) at the centre and highest at the walls.

Fig. 4(b) shows a reverse trend that is the dimensionless entropy generation is maximum at the centre, while it declines to minimum close to the wall. To explain this seemingly aberrant trend, it is to be understood that  $N_s = N_{RC} + N_{AC} + N_{FF}$  (see Eqs. (28-33)). For higher  $n$ ,  $N_{AC}$  is much higher than  $N_{RC}$  and  $N_{FF}$ , so the variation in  $N_s$  is influenced the most by variation in  $N_{AC}$ . If we look at

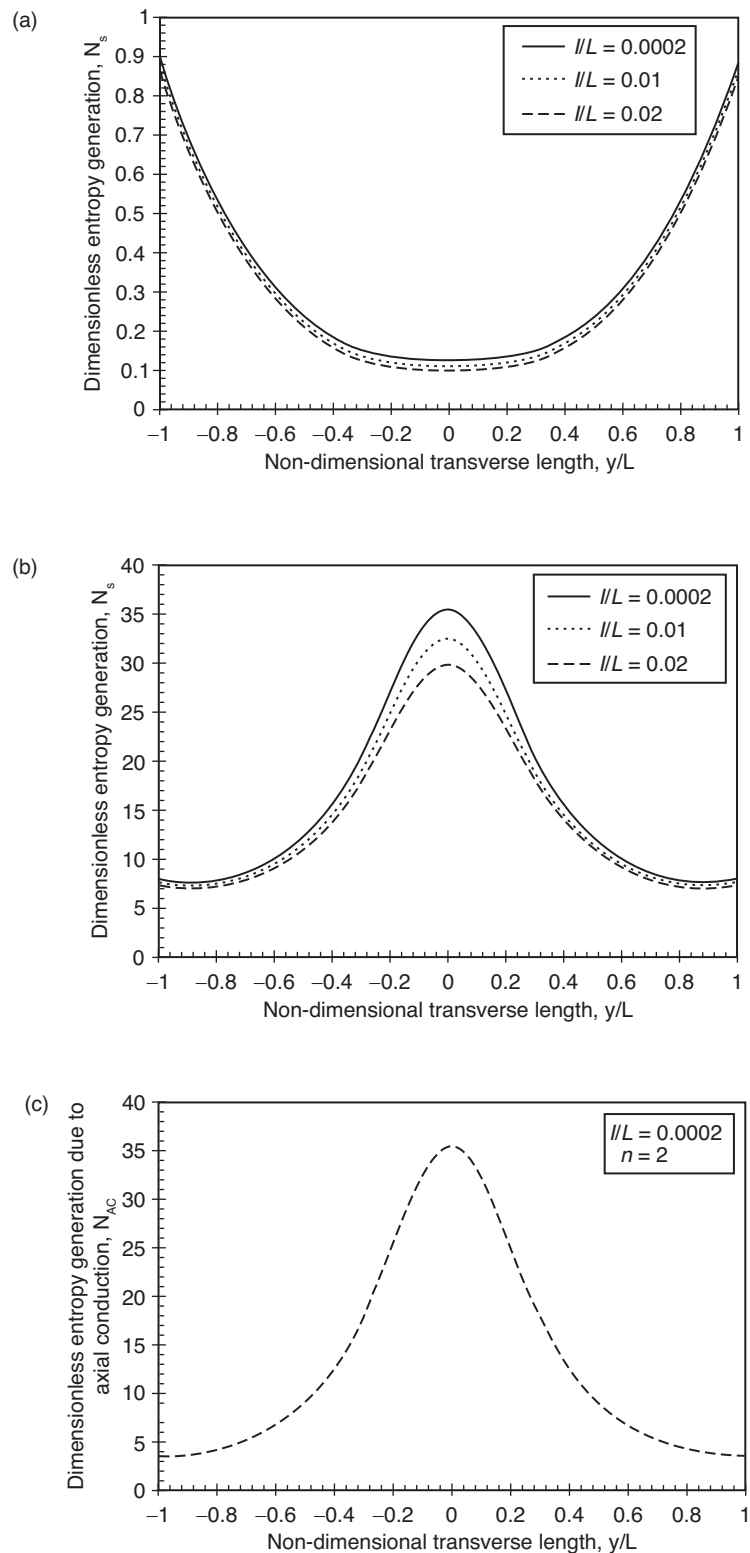


Figure 4. Variation of dimensionless entropy generation along the channel width at different  $l/L$  ratio for (a)  $n = 0.5$  (b)  $n = 2$  (c) Variation of dimensionless entropy generation due to axial conduction along the channel width ( $2l$ ) for  $l/L = 0.0002$  ( $l = 10\text{nm}$ ) and  $n = 2$

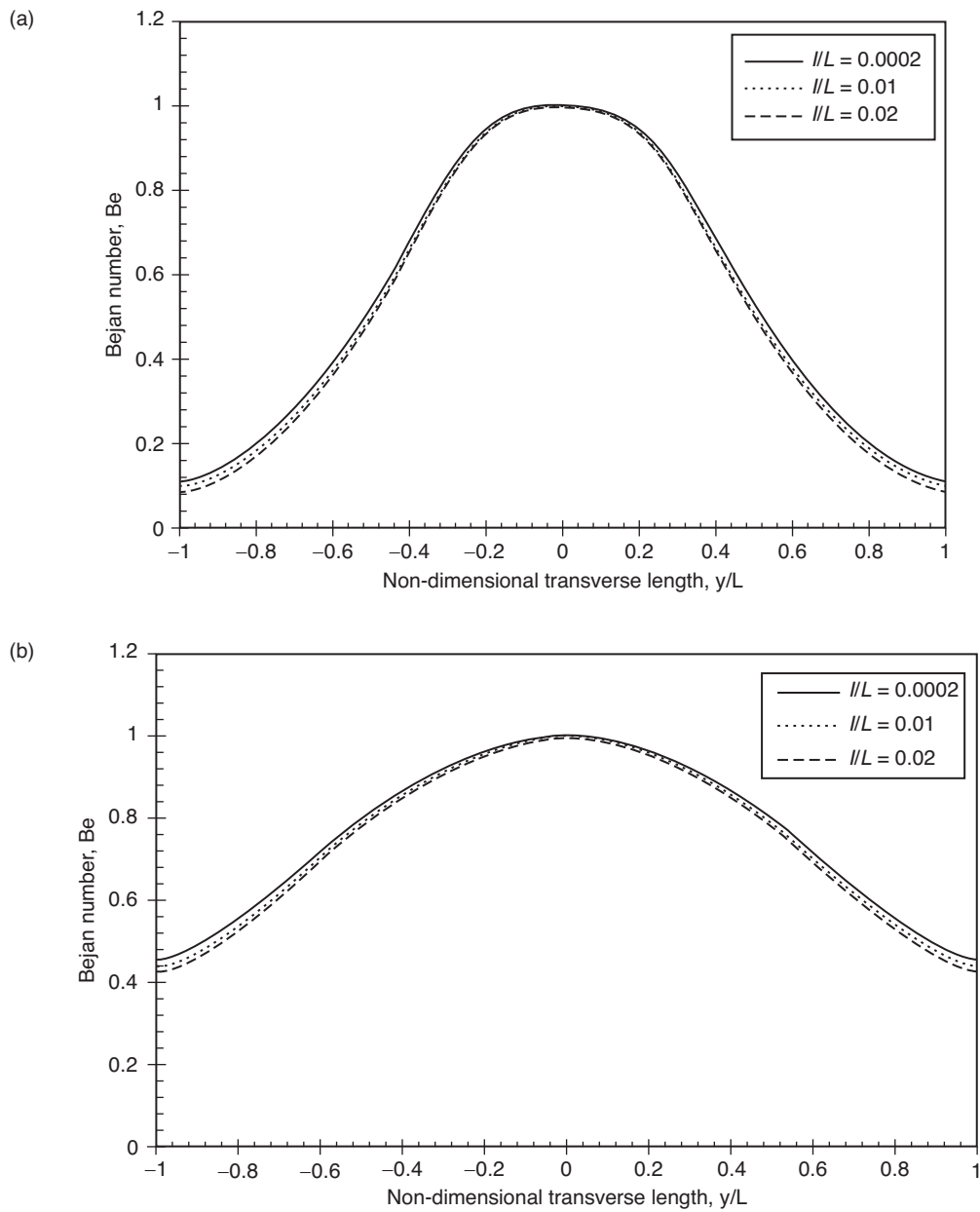


Figure 5. Variation of bejan number along the channel width at different //L ratio for (a)  $n = 0.5$  (b)  $n = 2$

Fig. 4(c), it clearly shows that  $N_{AC}$  tends to maximum at the centre. This increase in  $N_{AC}$  causes the overall entropy generation to increase at the center. This explains the trend seen in Fig. 4(b).

Also it is seen from Fig. 4(a) and Fig. 4 (b), that with increase in non dimensional slip length, the non dimensional entropy generation decreases. This can be explained as follows: as the //L increases, the non dimensional temperature gradient decreases (see Fig. 3), which leads to a decrease in entropy generation. Even though, as //L increases,  $du/dy$  increases (see Fig. 2), but the impact of this is compensated by the corresponding decrease in temperature gradient. In fact, for  $n = 2$ , the impact of //L on the entropy generation is more severe.

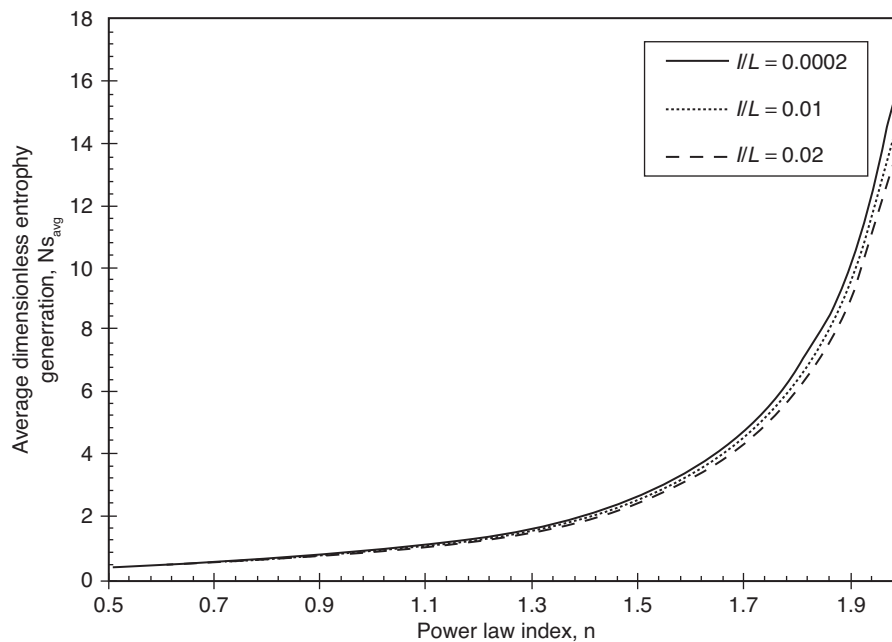


Figure 6. Variation of average dimensionless entropy generation with power law index for different  $l/L$  ratio

Figure 5(a) and 5(b) show the Bejan number along the channel width at different values of  $l/L$  ratio for pseudo plastic ( $n = 0.5$ ) and dilatant fluid ( $n = 2$ ), respectively. As can be seen from the figures,  $Be$  attains its maximum value of 1 at the centerline, while it is minimum at the walls. This is because the velocity gradient is 0 at the centre, so all the entropy generated at the center is due to heat transfer (temperature gradient). And the shear stress or the fluid friction is highest at the walls, so the  $Be$  is lowest there. Moreover with increase in  $l/L$ ,  $Be$  decreases for both pseudo plastic and dilatant fluids.

This can be explained as follows: the temperature gradient inside the fluid decreases with increase in  $l/L$  (see Fig. 3) which leads to a decrease in entropy generated due to temperature gradient and hence in  $Be$ .

Figure 6 shows the variation of area averaged dimensionless entropy generation with the power law index at different values of  $l/L$ . It can be seen from the figure that the average entropy generation increases with increase in power law index. This is expected because, as seen in Fig. 2 and Fig. 3, both the temperature gradient and the velocity gradient increase with increase in power law index. Moreover, the average dimensionless entropy generation decreases with increase in  $l/L$ . Again, this is expected because non dimensional entropy generation at a point decreases with increase in  $l/L$ , as shown in Fig. 4. Moreover, the effect of  $l/L$  on the average entropy generation is more pronounced for dilatant fluids ( $n > 1$ ) than for pseudo plastic fluids ( $n < 1$ ).

#### 4. CONCLUSIONS

The effect of slip length on dimensionless temperature distribution and dimensionless entropy generation, Bejan number and average entropy generation has been studied for power law fluid in a microchannel. Since the slip length affects the velocity distribution, which in turn is intimately linked to entropy generation, so the entropy generation is also intrinsically linked to slip length. It is observed that the temperature inside the channel increases while the dimensionless entropy generation and  $Be$  decrease with increase in slip length. The effect of slip length is more pronounced for dilatant fluids compared to pseudo plastic fluids. This is because in dilatant fluids, the contribution of fluid irreversibility to entropy generation is more pronounced. So the slip length must not be neglected for calculating entropy generation in dilatant fluids.

**REFERENCES**

- [1] C.L.M.H. Navier, 1827. “Memoire sur les lois du mouvement des fluides”, *Mem. Acad. Roy. Sci. Inst. Fr.* 6, pp. 389–440.
- [2] J.C. Maxwell, 1879. “On stresses in rarefied gases arising from inequalities of temperature”. *Philosophical Transactions of Royal Society of London*, 170, pp. 231–256.
- [3] L.L.Ferras, J.M. Nobrega, F.T.Pinho, 2012. “Analytical solutions for Newtonian and inelastic non-Newtonian flows with wall slip” 175–176, May, pp. 76–88.
- [4] A. Bejan, 2006. “Advanced Engineering Thermodynamics”, John Wiley and Sons, Hoboken.
- [5] S. Mahmud, R.A. Fraser, 2002. “Thermodynamic analysis of flow and heat transfer inside channel with two parallel plates” *Exergy*, 2(3), pp. 140–146.
- [6] S. Mahmud, R.A. Fraser, 2002. “Inherent Irreversibility of channel and fluid flow for non-Newtonian fluid”, *International Communications in Heat and Mass Transfer*. 29(5), July, pp. 577–587.
- [7] Y.M. Hung, 2008, “Viscous dissipation effect of entropy generation for non-Newtonian fluids in microchannel”, *International Communications in Heat and Mass Transfer*. 35(9), November, pp. 1125–1129.
- [8] A. Barletta, 1997, “Fully developed laminar forced convection in circular ducts for power-law fluids with viscous dissipation”, *International journal of Heat and Mass Transfer*. 40(1), pp. 655–666.
- [9] A. Bejan, 1995, “Entropy Generation Minimization” CRC Press, Boca Raton.
- [10] S. Paoletti, F. Rispoli, E. Sciubba, 1989. Calculation of exergetic losses in compact heat exchanger passages. ASME AES- 10, 21–29.

